Proc. Schl. Eng. Tokai Univ., Ser. E
42 (2017) 15-21

Research on Skid Control of Small Electric Vehicle (Effect of Velocity Prediction by Observer System)

by

Sean RITHY[*1] and Hirohiko OGINO[*2]

(Received on Apr. 5, 2017 and accepted on Jul. 6, 2017)

Abstract

In recent years, the vehicles using a motor as a power source increase. In particular, it is expected that a small electric vehicle increase in an urban area. However, a seat belt is an only safety equipment in most small electric vehicles. In particular, a small electric vehicle using In-Wheel Motor System as a driving unit has no space for Anti-Lock Braking System which is a basic skid control system. Then, the small electric vehicle will be easily in a dangerous or unstable condition on a wet or icy road. The purpose of this study is to improve the safety of small electric vehicles. We have studied the skid control of the small electric vehicle with In-Wheel Motor System. The vehicle velocity is needed to control the skid. However, the high accuracy measurement equipment of vehicle velocity is too expensive to install in a commercially vehicle. Then, we propose the skid control with the vehicle velocity predicted by observer system. The effect of the prediction of observer system was discussed in this paper.

Keywords: Small electric vehicle, Icy road, Skid control, Observer system

1. Introduction

According to increasing of the green products consumption, the automobile manufacturers have been researching on hybrid vehicles or electric vehicles to improve the safety performance, controllability and stability. An electric vehicle is the green product and a small electric vehicle (SEV) is more convenience in urban area. For example, Guideline to Introduce Super Small Mobility[1)] of Ministry of Land, Infrastructure and Transport of JAPAN predicted the future mobility in urban area will be SEV.

SEV has two types of motor system which are type one is one motor system and type two is In-Wheel Motor System (IWMS) which attached the electric motor in driving tire rim. We think that IWMS will generally be used in SEV because it has no transmission and power transfer system. Then, IWMS has low energy loss, quick torque response and ability to a measure the torque applied on each tire[2)]. The question we have to ask here is whether SEV with IWMS has enough safe. IWMS of SEV has some defect points which the volume of tire housing is small, then the heat problem is easily occurred. There is no space in tire rim to install the hydraulic brake actuator, thus Anti-Lock Braking System (ABS) not adapted. ABS is a basic skid control system, and ABS is adopted to almost all standard size vehicles. On the other hand, the seat belts are the only safety equipment of most SEV. Then, we can say the safety of SEV is not enough. The purpose of this study is to improve the safety of small electric vehicles. Most of previous studies on skid control of an electric vehicle is based on slip ratio. In that methods, the vehicle velocity needs to be measured or estimated for the calculation of the slip ratio[3)-5)]. However, measuring the accurate value of vehicle velocity is too difficult or the high accuracy measurement equipment of vehicle velocity is too expensive to install in a commercially vehicle. For example, Heerwan et al researched about the skid control of SEV[6)]. They used the vehicle velocity of vehicle model. Then, we propose the skid control with the vehicle velocity predicted by observer system. In this report, we would like to examine the effects of observer system control in the straight and turning brake motion by the simulation.

*1 Graduate student, Course of Mechanical Engineering
*2 Professor, Department of Prime Mover Engineering

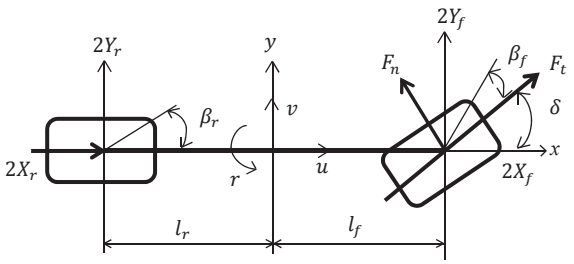

Fig. 1 Two-wheel vehicle model

2. Analysis

2.1 *Main symbol*

F: braking force [N], *f*: friction force [N], *g*: gravitational acceleration [m/s^2], *h*: gain to reduce the error, *I*: moment of inertia [kgm^2], *K*: cornering rigidness [N/rad], *m*: body mass [kg], *P*: braking pressure [Pa], *R*: tire radius [m], *r*: yaw angular velocity [rad/s], *s*: laplace operator, *T*: torque [Nm], *u*: vehicle longitudinal speed [m/s], *v*: vehicle lateral speed [m/s], *W*: tire load [kg], *x*: co-ordinate in the longitudinal direction, *X*: force along to x axis, *y*: co-ordinate in the lateral direction, *Y*: force along y axis, β: side slip angle [rad], ρ: slip ratio, μ: friction coefficient, ω: tire angular velocity [rad/s], δ: steering angle [rad].

Suffix:

n: normal direction, *t*: tangential direction, *f*: front tire, *r*: rear tire, *: predicted

2.2 *Simulation model*

The following points were assumed.

1) The tire characteristics of left and right tires are same.

2) The tire load movements from inner tires to outer tire in turning motion is negligible.

From these assumptions, the vehicle modeled by the two-wheel vehicle model. Figure 1 shows the two-wheel vehicle model.

2.3 *Basic equations of motion*

The velocities *u*, *v* along *x* and *y* axis and the yaw angular velocity *r* are calculated by following dynamic equations.

$$m\left(\frac{du}{dt} - v\,r\right) = 2\,(X_f + X_r) \quad (1)$$

$$m\left(\frac{du}{dt} + u\,r\right) = 2\,(Y_f + Y_r) \quad (2)$$

$$I\left(\frac{dr}{dt}\right) = 2\,(l_f Y_f - l_r Y_r) \quad (3)$$

The forces of these equations are obtained from tire model mentioned in the next chapter.

2.4 *Tire model*

The coulomb tire model was used to obtain the friction force. Then, the force F_t and X_r were calculated by following equations.

$$F_t = \mu_f W_f \quad (4)$$

$$X_r = \mu_r W_r \quad (5)$$

The friction coefficient was calculated by Magic formula [7].

$$\mu_{f,r} = -1.1 C_{road}\left(e^{-35\rho_{f,r}} - e^{-0.35\rho_{f,r}}\right) \quad (6)$$

The road coefficient C_{road} was,

for dry asphalt $C_{road} = 0.8$

for icy road $C_{road} = 0.12$

The slip ratio can be presented in terms of the traction between the road and the tire surface, which is defined as:

$$\rho_{f,r} = \frac{u^* - R\omega_{f,r}}{u^*} \quad (7)$$

Where the predicted vehicle velocity u^* obtained by observer system.

The cornering force F_n and Y_r were calculated by the liner tire model as following equation.

$$F_n = -K_f \beta_f \quad (8)$$

$$Y_r = -K_r \beta_r \quad (9)$$

The side slip angles of front and rear tires was calculated as follows,

$$\left.\begin{aligned} \beta_f &= \tan^{-1}\left(\frac{v + r l_f}{u}\right) - \delta \\ \beta_r &= \tan^{-1}\left(\frac{v - r l_r}{u}\right) \end{aligned}\right\} \quad (10)$$

The forces X_f and Y_f are calculated as follows,

$$X_f = F_t \cos\delta - F_n \sin\delta \quad (11)$$

$$Y_f = F_t \sin\delta + F_n \cos\delta \quad (12)$$

3. State observer system

3.1 *Linear model*

The state observer system uses linear model dynamic equation of translation motion and yaw angular velocity such as[7]:

$$V\left(\frac{d\beta^*}{dt} + r^*\right) = 2Y_f + 2Y_r \quad (13)$$

$$I\frac{dr^*}{dt} = 2l_f Y_f - 2l_r Y_r \quad (14)$$

$$\frac{du^*}{dt} = \frac{1}{m}\left(2X_f + 2X_r\right) + r^* u^* \beta^* \quad (15)$$

The predicted side slip angle of gravity center and yaw angular velocity, $\beta^*$and r^* were obtained from equation (13) and

(14). Inserted these predicted values to equation (15). Then, the predicted vehicle velocity $u*$ was obtained from equation (15).

3.2 *Linearized differential equation*

The linear dynamic equations were obtained from the differential equations (13) and (14). The non-linear terms were the forces Y_f and Y_r. We assume the side slip angles were small. Then,

$$Y_f = -K_f\beta_f = -K_f\left(\beta^* + \frac{l_f r^*}{v^*} - \delta\right) \quad (16)$$

$$Y_r = -K_r\beta_r = -K_r\left(\beta^* - \frac{l_r r^*}{v^*}\right) \quad (17)$$

Substitute equation (16) and equation (17) into equation (13) and equation (14) gives the following:

$$\frac{d\beta^*}{dt} = \frac{1}{mu^*}\left[2K_f\delta - 2(K_f + K_r)\beta^* - \left\{mu^* + \frac{2}{u^*}(l_fK_f - l_rK_r)\right\}r^*\right] \quad (18)$$

$$\frac{dr^*}{dt} = \frac{1}{I}\left[2l_fK_f\delta - 2(l_fK_f - l_rK_r)r^* - \frac{2(l_f^2K_f + l_r^2K_r)}{u^*}r\right] \quad (19)$$

Now extent the equation (18) and equation (19)

$$\frac{d\beta^*}{dt} = -\frac{2(K_f + K_r)}{mu^*}\beta^* - \left\{1 + \frac{2}{mu^{*2}}(l_fK_f - l_rK_r)\right\}r^* + \frac{2K_f}{mu^*}\delta \quad (20)$$

$$\frac{dr^*}{dt} = -\frac{2(l_fK_f - l_rK_r)}{I}\beta^* - \frac{2(l_f^2K_f + l_r^2K_r)}{u^*I}r + \frac{2l_fK_f}{I}\delta \quad (21)$$

Put some terms as follows:

$$\left.\begin{aligned} G_1 &= -\frac{2(K_f + K_r)}{mV} \\ G_2 &= -\left[1 + \frac{2}{mu^{*2}}(l_fK_f - l_rK_r)\right] \\ G_3 &= \frac{2k_f}{mu^*} \\ H_1 &= -\frac{2(l_fK_f - l_rK_r)}{I} \\ H_2 &= -\frac{2(l_f^2K_f + l_r^2K_r)}{u^*I} \\ H_3 &= \frac{2l_fK_f}{I} \end{aligned}\right\} \quad (22)$$

Thus, equations are expressed:

$$\left.\begin{aligned} \frac{d\beta^*}{dt} &= G_1\beta^* + G_2r^* + G_3\delta \\ \frac{dr^*}{dt} &= H_1\beta^* + H_2r^* + H_3\delta \end{aligned}\right\} \quad (23)$$

It is arranged as system equations in the vector state form:

$$\mathbf{X} = \begin{bmatrix}\beta^* \\ r^*\end{bmatrix} \quad (24)$$

$$\mathbf{A} = \begin{bmatrix}G_1 & G_2 \\ H_1 & H_2\end{bmatrix} = \begin{bmatrix}-\frac{2(K_f + K_r)}{mu^*} & -1 - \frac{2}{mu^{*2}}(l_fK_f - l_rK_r) \\ -\frac{2(l_fK_f - l_rK_r)}{I} & -\frac{2(l_f^2K_f + l_r^2K_r)}{u^*I}\end{bmatrix} \quad (25)$$

$$\mathbf{B} = \begin{bmatrix}G_3 \\ H_3\end{bmatrix} = \begin{bmatrix}\frac{2K_f}{mu^*} \\ \frac{2l_fK_f}{I}\end{bmatrix} \quad (26)$$

$$\dot{\mathbf{X}} = \mathbf{A}\mathbf{X} + \mathbf{B}\delta \quad (27)$$

$$\left.\begin{aligned} \beta^* &= \mathbf{C_1^T}\dot{\mathbf{X}} \\ r^* &= \mathbf{C_2^T}\dot{\mathbf{X}} \end{aligned}\right\} \quad (28)$$

$$\left.\begin{aligned} \mathbf{C_1^T} &= [1 \quad 0] \\ \mathbf{C_2^T} &= [0 \quad 1] \end{aligned}\right\} \quad (29)$$

4. Control method

Figure 2 shows the control flow chart. We employed the two control methods of braking pressure to skid control. The 1st control method of skid control was same as Heerwan et al[6]. The pressure controller controlled the braking pressure based on optimum range of slip ratio to maintain the maximum value of friction coefficient. Heerwan et al[6] used the vehicle velocity from vehicle model. On the other hand, in this research, the vehicle velocity was predicted from observer system. The predicted slip ratio ρ_r^* and ρ_f^* were calculated by the rotation speed of each tire from vehicle and predicted vehicle velocity $u*$. The pressure controller controls the braking pressure to maximize the friction coefficient. The 2nd method is the output feedback. The basic equations of observer system were simple because it had to predict the vehicle velocity at high speed. Then, the predicted velocity value included an error. Therefore, the following method was used to reduce the error. We focused the yaw angular velocity that could measure relatively easily. Then, the error of yaw angular velocity was calculated by the information from vehicle and from observer system. The product of gain h and the error was feedback to the input.

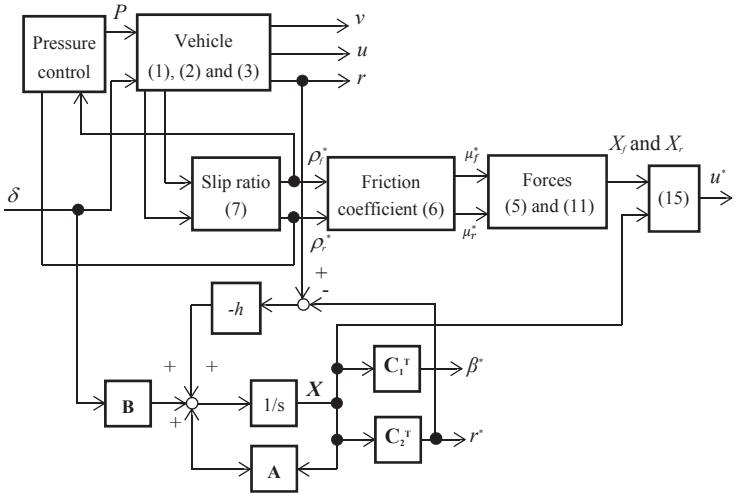

Fig. 2 Control flow chart

5. Calculate condition

The specifications of the model were same as COMS (AK10E) made by TOYOTA BODY Co. Figure 3 shows the image of COMS. Table 1 shows the main specifications of COMS. The following two cases were performed and the three examinations were performed in each cases. The first examination was no skid control. This results were the standard to clear the effect of the skid control and observer system. The second examination was the skid control which used the velocity of vehicle model. The third examination was the skid control which used the predicted velocity of observer system.

At first, the straight braking motion was simulated. The initial vehicle speed was 40Km/h. The road condition was icy road. Next, the turning braking motion was simulated. The steering angle of front tire is 10 degrees. The initial velocity was 40km/h.

6. Results and discussions

6.1 *Straight braking motion*

The proposed observer system used the error of yaw angular velocity to reduce the error of predicted velocity u^*. However, the yaw angular velocity is zero at straight braking motion. Then, there is no feedback information from the vehicle to observer system in straight braking motion. For this reason, we showed the effect of observer system for the skid control. Figure 4 shows the velocity change on the icy road. When the skid was not controlled, the vehicle needed the long time to stop.

Figure 5 and Fig. 6 show the change of slip ratios and friction coefficients of the no skid control case. The front and rear slip ratios increased to 1.0. These meant the rotation speeds of front tire and rear tire became to zero. Then, the friction coefficients had low values and the stoppage time was long. The reason why the slip ratio of front tire became to 1.0 in a short time was that the inertial moment of front tire was small. The rear tire connected to the driving motor, then the inertial moment of rear tire was larger than the front tire.

Figure 7 and Fig. 8 show the change of slip ratios and friction coefficients of the skid control with vehicle velocity information. The slip did not increase 1.0, then, the friction coefficients were maintained the large values. Therefore, the stoppage time became short.

From Fig. 4, in neither the velocity from the vehicle nor the velocity from observer system, the stoppage time had a small difference. Then, the error of velocity and error of slip ratio defined as following equations were obtained.

$$e_\rho = \frac{\rho - \rho^*}{\rho} \times 100\% \qquad (31)$$

$$e_u = \frac{u - u^*}{u} \times 100\% \qquad (30)$$

Where, u and ρ were the vehicle velocity and slip ratio from vehicle, u^* and ρ^* were the predicted velocity and slip ratio from observer system.

Fig. 3 TOYOTA COMS

Table 1 Parameter for TOYOTA COMS

Parameter	Symbol	Value	Unit
Inertial motion	I	1000	kgm^2
Front tire inertia	I_f	2.53	kgm^2
Rear tire inertia	I_r	0.43	kgm^2
Front corning rigidness	K_f	$3.33x10^6$	N/m^3
Rear corning rigidness	K_r	$3.33x10^6$	N/m^3
Length from gravity to the front tire	l_f	0.84	m
Length from gravity to the rear tire	l_r	0.815	m
Body mass	m	422	kg
Tire radius	R	0.23	m

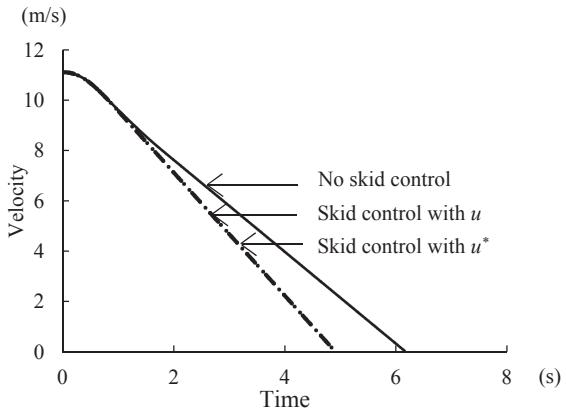

Fig. 4 Comparison time change of velocity

Figure 9 shows the change of e_u. Though the velocity became near zero just before the vehicle stop, the braking pressure controlled to maximum value and zero, then the e_u had large value. But the maximum value of e_u is 0.11%.

Figure 10 shows the change of e_ρ. The slip ratio error e_ρ had the large value at immediately after the start of baking, the t=0, and at the stop moment. The slip ratio ρ had small value at the start of braking, then the e_ρ had the large value. The reason of increase of e_ρ at the stop moment was the e_u increase at that time. Then it is reasonable to suppose that the predicted velocity of observer system has the enough predictability in the straight braking motion.

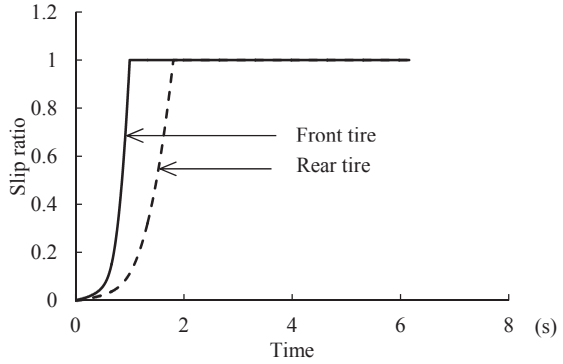

Fig. 5 Time change of slip ratio of no skid control

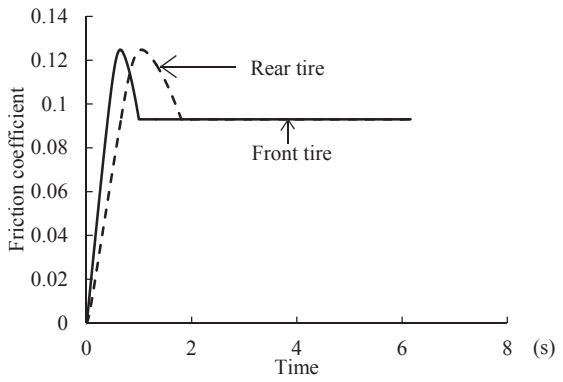

Fig. 6 Time change of friction coefficient

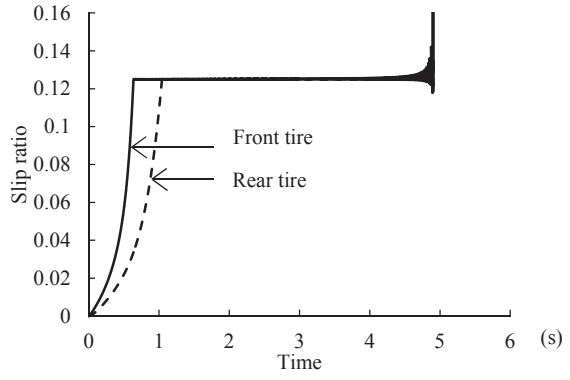

Fig. 7 Time change of slip ratio of skid control with u

6.2 *Turning braking motion*

(1) The vehicle motion with no skid control

Before we show the effect of the proposed observer system, it will be useful to discuss the vehicle motion with no skid control in turning brake motion.

Figure 11 shows the trajectory of the vehicle on icy road. The steer angle was 10 degrees and the initial velocity was the 40km/h. The road condition was icy. The vehicle started the left turning, but changed a turning direction from the point A, around lateral direction 12.5m and vertical direction 5m into the right. The reason why the vehicle direction changed to left turn to right was that the effect of side force of front tire was larger than the rear tire.

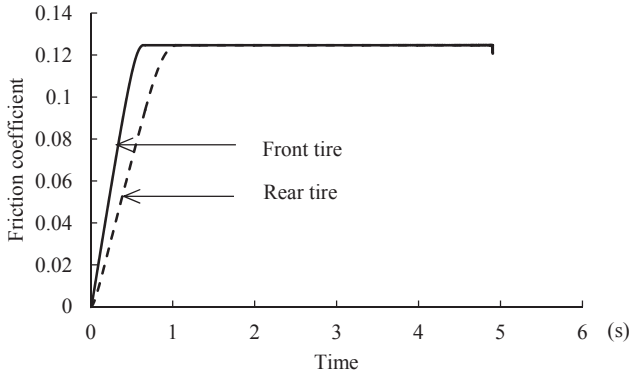

Fig. 8 Time change of friction coefficient of skid control with u

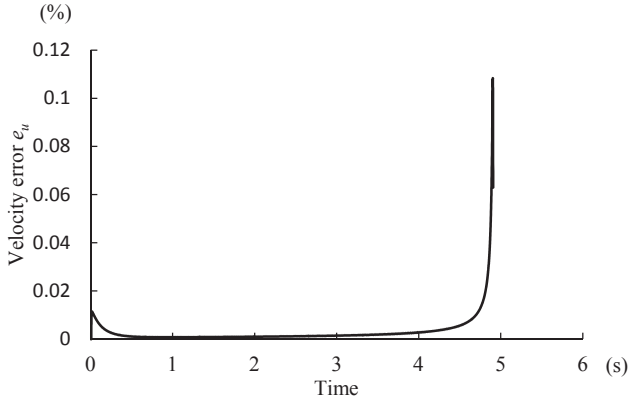

Fig. 9 Time change of velocity error e_u

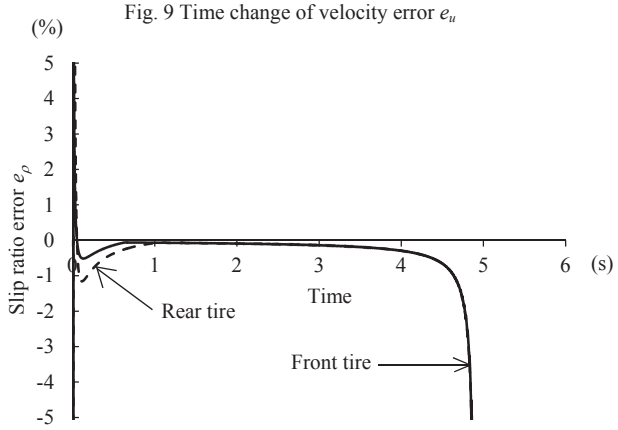

Fig. 10 Time change of slip ratio error e_ρ of front and rear tire

Figure 12 shows the change of the slip ratios. The front slip ratio became 1.0 early in comparison with rear slip ratio. The inertial moment of front tire was smaller than the inertial moment of rear tire, then the rotation speed of front tire decreased quickly, and the slip ratio increased quickly. The friction force and the side force acted on the tire, but the friction force reduced according to the reduction of the slip ratio. Therefore, the effect of the side force of front tire gradually became large for the rear tire. On the other word, the force vector that was the resultant of the friction force and the side force acted on the front tire was rotate to the lateral direction. When the direction of the resultant force reversed, the vehicle direction changed to opposite direction.

Figure 13 shows the change of velocities. The simulation was stopped when the longitudinal velocity u became zero. At that time, the lateral velocity was not zero, this meant the vehicle moved to lateral direction. The direction change and the lateral movement mean this vehicle became the unstable condition what was called "spin".

(2) The effect of the proposed observer system

It is difficult to use the measuring of vehicle velocity as mentioned before, but the skid control use the vehicle velocity is the most effective control. Then, we compared the effect of observer system with the cases those were the no control and the skid control by the vehicle velocity. The notations of "the vehicle velocity" and "observer system velocity" in following descriptions meant "The skid control by the measured vehicle velocity u." and "The skid control by the predicted velocity u^* of proposed observer system". The trajectories of skid control cases those are both of the vehicle velocity and observer system velocity became the arks from Fig. 11. The turning radius became slightly large by observer system velocity.

Figure 14 shows the changes of velocities. The longitudinal velocity and the lateral velocity of both cases became zero at the same time, then, vehicle stopped in the stable condition without skidding. However, the stoppage time of observer system velocity was almost same as the no control. The cause of the increase of stoppage time of observer system velocity was the error of the predicted velocity u^*.

Figure 15 shows the vehicle velocity u and the predicted velocity u^*. Note these velocities are simulation results of observer system velocity case. The vehicle velocity u was from the vehicle model and observer system velocity from observer system in the same simulation model. The predicted velocity u^* was decrease rapidly than the vehicle velocity u. And the predicted velocity u^* reached to zero. This meant the observer system judged the vehicle stopped. Then, observer system became uncontrollable the skidding motion.

Therefore, the stoppage time was increase. The vehicle velocity u was relatively small at the predicted velocity u^* reached at zero, then, the vehicle stopped in stable. However, it may be in an unstable condition when the disturbance is input just before a stop. Therefore, it is necessary to improve predictive precision, but we examine this problem and want to report it next time.

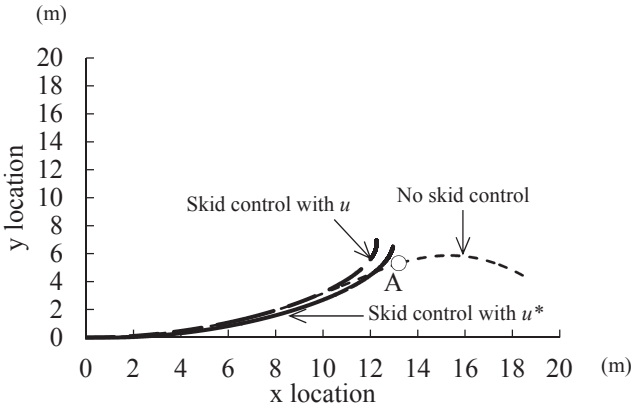

Fig. 11 Comparison time change of trajectory

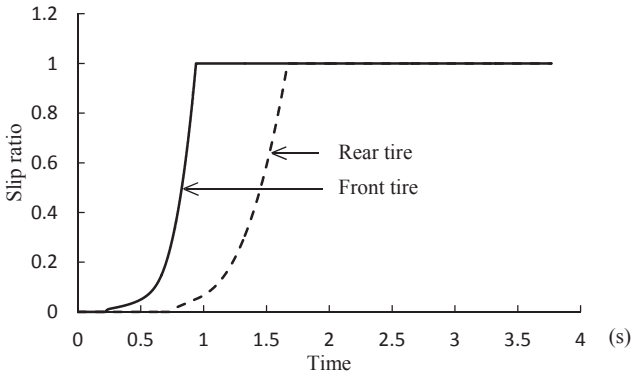

Fig. 12 Comparison time change of slip ratio

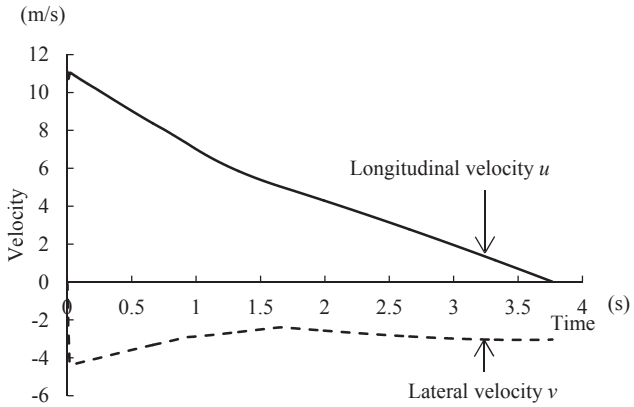

Fig. 13 Comparison time change of longitudinal velocity and lateral velocity

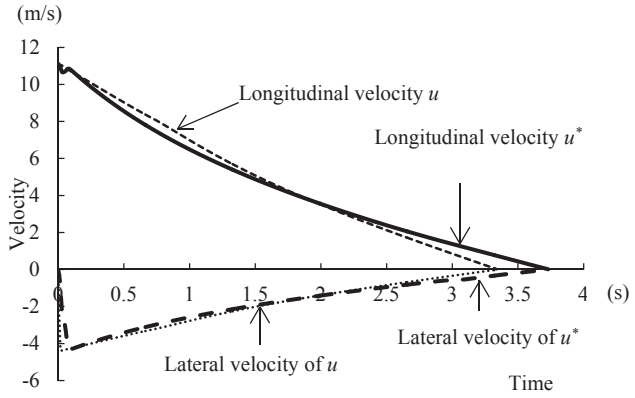

Fig. 14 Comparison time change of longitudinal velocity and lateral velocity of vehicle and observer system

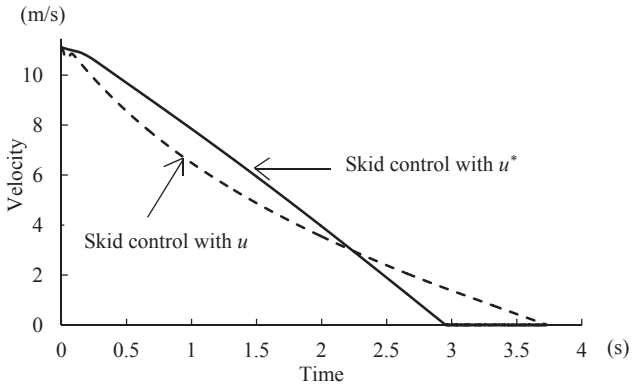

Fig. 15 Comparison time change of velocity u and u^*

7. Conclusion

We propose the skid control with the vehicle velocity predicted by observer system. The effect of the prediction of observer system was discussed. We had the following conclusions.

(1) The straight brake motion.

The stoppage time of vehicle that the skid was controlled by the proposed observer system on icy road was almost same as the result that controlled by vehicle information. And the prediction errors of velocity and slip ratio were small. Then it is reasonable to suppose that the predicted velocity of observer system has the enough predictability in the straight braking motion.

(2) The turning brake motion.

The vehicle with the skid control of observer system stop in the stable condition on icy road. However, the stoppage time of the observer velocity was almost same as the no control. The cause of the increase of stoppage time of the observer velocity was the error of the predicted velocity.

References

1) Ministry of Land, Infrastructure and Transport Department Municipal Affairs Bureau, Automobiles of Japan: *Guideline for introduction to Utra-Compact Mobility, Japan* (2013) http://www.mlit.go.jp/common/000212867.pdf(in Japanese)

2) K. Fujii and H. Fujimoto: Traction Control Based on Slip Ratio Estimation without Detecting Vehicle Speed for Electric Vehicle, Proceedings of the 2007 Power Conversion Conference, pp.688-693, (2007)

3) Cai, Z., Ma, Z. and Zhao, Q.: Acceleration-to-torque ratio based anti-skid for electric vehicle, Proceedings of the 2010 IEEE International Conference on Mechatronics and Embedded Systems and Applications (2010), pp.577-581

4) Hasegawa, S. and Ogino H.: Research on skid control of small electric vehicle with hydraulic-mechanical hybrid brake system(1st Report: Simulation of 2 wheel model of anti-lock braking system), Proceeding of the School of Engineering, Tokai University, 49, No.2(2009), pp.89-94 (in Japanese)

5) Sakai, S., Sado, H. and Hori, Y.: Anti skid control with motor in electric vehicle, Proceedings of the 6th International Workshop on Advanced Motion Control (2000), pp.317-322.

6) Mohamad Heerwan Bin Peeie, H. Ogina: Research on Skid Control of Small Electric Vehicle with Hydraulic-Mechanical Hybrid Brake System, proceeding of INTERNATIONAL CONFERENCE ON SUSTAINABLE MOBILITY 2010, (CD-ROM)

7) Masato Abe: *Vehicle Handling Dynamics, Theory and Application second edition (fundamentals of vehicle dynamics)*, Kanagawa Institute of Technology Publication, pp.51, 2015